

Temperature phase transition and an effective expansion parameter in the $O(N)$ -model

M. BORDAG*

University of Leipzig, Institute for Theoretical Physics
Augustusplatz 10/11, 04109 Leipzig, Germany

and

V. SKALOZUB†

Dnepropetrovsk National University, 49050 Dnepropetrovsk, Ukraine

October 18, 2018

Abstract

The temperature phase transition in the N -component scalar field theory with spontaneous symmetry breaking is investigated in the perturbative approach. The second Legendre transform is used together with the consideration of the gap equations in the extrema of the free energy. Resummations are performed on the super daisy level and beyond. The phase transition turns out to be weakly of first order. The diagrams beyond the super daisy ones which are calculated correspond to next-to-next-to-leading order in $1/N$. It is shown that these diagrams do not alter the phase transition qualitatively. In the limit N goes to infinity the phase transition becomes second order. A comparison with other approaches is done.

1 Introduction

The temperature induced phase transition in the N -component scalar field theory ($O(N)$ -model) has been investigated by many authors. The interest to this problem results, in particular, from the importance of the spontaneous symmetry breaking and symmetry restoration at finite temperature in various modern field theoretical models of elementary particles including different content of scalar fields. The present status of this problem is characterized by a general opinion

*e-mail: Michael.Bordag@itp.uni-leipzig.de

†e-mail: Skalozub@ff.dsu.dp.ua

that the phase transition in the $O(N)$ -models (including $N=1$) is of second order (see, for instance, the standard text books [1, 2, 3].) This conclusion results mainly from the non perturbative methods - lattice simulations, average action (flow equation) methods, large- N expansion [4, 5, 6, 7, 8]. In opposite, a first order phase transition was found in the most perturbative approaches [9, 10, 11]. Here, the key problem - the necessity of resummation of the infrared divergences of a series in the coupling constant - has been overcome by applying the super daisy resummation. However, after that another problem - the lack of the smallness of the effective expansion parameter near the phase transition - remains. This observation prevents conclusive results from the resummed perturbation theory and it leaves room for the expectation that a further resummation of the perturbation expansion is able to weaken the first order character of the expansion making it a second order at the end. In recent papers [12, 13] by an auxiliary-mass method it was found that the phase transition in either the $O(1)$ - or the $O(N)$ -model is of second order. Moreover, it was also stated in Ref. [12] that in perturbation theory at the two-loop level the phase transition is also of second order when diagrams beyond the super daisy type are taken into account. Because of the importance of these results we shall discuss them in more detail in what follows. Here, we note that the effective potential calculated by this method has an imaginary part in its minimum which means an inconsistency of the calculation procedure adopted.

In our previous paper [14] within the $O(1)$ -model we developed as a new method the combination of the gap equation resulting from the second Legendre transform with the condition of the free energy considered as a function of the condensate to be in an extremum. This allows for the exclusion of the condensate value from the gap equation and results in considerable simplifications. For instance, in the super daisy approximation we obtained very simple explicit formulas showing clearly a first order phase transition. We applied our method to a certain class of graphs beyond this approximation and obtained an increase of the first order character of the transition.

In the present paper we generalize our method to the $O(N)$ -model. Again, in the extrema of the free energy, we exclude the condensate from the gap equations which form a set of two equations for the Higgs and Goldstone field masses. We consider in detail both, the super daisy resummation and the next class of graphs beyond. We find that the phase transition is of first order for any finite N turning into a second order one in the limit of N goes to infinity. At the same time, the observed phase transition is very close to a second order one and differs from it in the next-to-leading order in $1/N$ for finite but large N . We demonstrate the effectiveness of our method by calculating a certain class of graphs beyond the super daisy approximation in the $O(N)$ -model, namely those which correspond to the next-to-next-to-leading order for large N . Here we are left with a mostly numerical approach to the gap equations confirming the qualitative stability of our previous results. The diagram mentioned in Ref. [12] is also included in the carried out resummations. Its influence is discussed in the last section.

The paper is organized as follows. In the next section we collect the basic formulas of the resummation method based on the second Legendre transform together with our method to consider the gap equations in the extrema of the free energy. In the third section we consider the case corresponding to the super daisy approximation. In the fourth section the summation of the bubble chain diagrams is carried out. Conclusions are drawn in the last section. Some technical material is banned into the appendix.

2 Basic formulas

We consider a scalar N -component field theory in $(3 + 1)$ dimensions in the Euclidean space-time. The action reads

$$S[\phi] = \int dx \left(\frac{1}{2} \phi(x) \mathbf{K} \phi(x) - \frac{\lambda}{4N} (\phi(x))^4 \right), \quad (1)$$

where $\mathbf{K} = \square - m^2$ is the kernel of the free action. The sign is chosen so that the vacuum Green functions are given by the functional representation

$$Z \equiv e^W = \int D\phi e^S, \quad (2)$$

where W is the functional of the connected Green functions. It is connected by the relation

$$W = -FT \quad (3)$$

with the free energy F . We consider the theory at finite temperature T in the Matsubara formalism so that the loop integrations are given by

$$Tr_p = T \sum_{l=-\infty}^{\infty} \int \frac{d^3 \vec{p}}{(2\pi)^3} \quad (4)$$

with the momentum $p = (2\pi Tl, \vec{p})$ ($l \in Z$). The symbol ϕ is here a condensed notation for N scalar fields, $\phi = \{\phi_1, \phi_2, \dots\}$. In the action Eq.(1) the following summation over the internal indices is assumed: $\phi^2 = \sum_{a=1}^N \phi_a^2$ and $\phi^4 = \left(\sum_{a=1}^N \phi_a^2 \right)^2$. In the present paper, we perform a standard renormalization procedure at zero temperature.

The second Legendre transform is introduced as follows. Consider as an arbitrary functional argument the full propagator β , instead of being the free one

$$\Delta = -K^{-1}, \quad (5)$$

Then the functional W is a functional depending on β : $W[\beta]$. Here and in the following we denote a functional dependence by squared brackets in opposite to the dependence of a function on its argument. So, for example, in momentum

representation, β is a function of the momentum p : $\beta(p)$, Whereas $W[\beta]$ is not, of course. In this sense the action Eq.(1) is also a functional of ϕ : $S[\phi]$.

Now, the second Legendre transform results in the representation

$$W = S[0] + \frac{1}{2}Tr \log \beta - \frac{1}{2}Tr \Delta^{-1} \beta + W_2[\beta] \quad (6)$$

of the connected Green functions, where β is subjected to the Schwinger-Dyson (SD) equation

$$\beta^{-1}(p) = \Delta^{-1} - \Sigma[\beta](p). \quad (7)$$

Here, $\Sigma[\beta](p)$ is the functional of all self energy graphs with no propagator insertions,

$$\Sigma[\beta](p) = 2 \frac{\delta W_2}{\delta \beta(p)}, \quad (8)$$

where δ is the functional derivative, see, e.g., [15] for details. $W_2[\beta]$ is the sum of all two particle irreducible (2PI) graphs taken out of the connected Green functions,

$$W_2[\beta] = \sum_{\text{2PI-graphs}} W[\beta] \quad (9)$$

with the function $\beta(p)$ on the lines.

The above formulas are written in condensed notations. So, they are valid for any theory with any number of fields. Below, we will write down them explicitly in the $O(N)$ -model. But before doing that we introduce the spontaneous symmetry breaking by turning the sign of the mass term in the free propagator, $m^2 \rightarrow -m^2$ in Δ so that it reads now $\Delta = p^2 - m^2$ in the momentum representation. Then, on the tree level, the minimum of the energy is on the shifted fields, $\phi_1 \rightarrow \eta + v$, where v is the field condensate. After that we change the notations according to $\{\phi_1, \phi_2, \dots\} \rightarrow \{\eta + v, \phi_1, \phi_2, \dots\}$ where η is the Higgs field and $\{\phi_1, \phi_2, \dots\}$ ($a = 1, 2, \dots, N - 1$) are the Goldstone fields which are symmetric under the residual $O(N - 1)$ symmetry.

In terms of the new variables the action reads

$$\begin{aligned} S[\eta, \Phi] = \int dx \left\{ \frac{m^2}{2} v^2 - \frac{\lambda}{4N} v^4 + \eta(m^2 - \frac{\lambda}{N} v^2) v \right. \\ \left. + \frac{1}{2} \eta(\square - \mu_\eta^2) \eta + \frac{1}{2} \phi(\square - \mu_\phi^2) \phi \right. \\ \left. - \frac{\lambda}{4N} (\eta^4 + 4\eta^3 v + 2(\eta^2 + 2\eta v) \phi^2 + \phi^4) \right\} \quad (10) \end{aligned}$$

with $\mu_\eta = -m^2 + 3\frac{\lambda}{N}v^2$ and $\mu_\phi = -m^2 + \frac{\lambda}{N}v^2$. Again, the summation over the internal indices is assumed. In momentum representation, the corresponding free propagators are

$$\Delta_\eta = p^2 + \mu_\eta^2 \quad \text{and} \quad \Delta_\phi = p^2 + \mu_\phi^2. \quad (11)$$

The propagator for the Goldstone fields is diagonal, $(\Delta_\phi)_{ab} = \delta_{ab} \Delta_\phi$. With these notations, the representation (6) for the connected vacuum Green functions takes the form

$$W = S[0] + \frac{1}{2} \text{Tr} \log \beta_\eta + \frac{N-1}{2} \text{Tr} \log \beta_\phi - \frac{1}{2} \text{Tr} \Delta_\eta^{-1} \beta_\eta - \frac{N-1}{2} \text{Tr} \Delta_\phi^{-1} \beta_\phi + W_2[\beta_\eta, \beta_\phi], \quad (12)$$

where $W_2[\beta_\eta, \beta_\phi]$ is the sum of all 2PI graphs with the propagators β_η and β_ϕ on the lines corresponding to the fields η and ϕ . In the $O(N)$ -model, the SD-equations form a set of N equations which are equivalent to one equation due to the symmetry. In the considered case of the broken symmetry, two equations remain:

$$\begin{aligned} \beta_\eta^{-1}(p) &= \Delta_\eta^{-1} - \Sigma_\eta[\beta_\eta, \beta_\phi](p), \\ \beta_\phi^{-1}(p) &= \Delta_\phi^{-1} - \Sigma_\phi[\beta_\eta, \beta_\phi](p), \end{aligned} \quad (13)$$

where following (8) the self energy functionals are given by

$$\begin{aligned} \Sigma_\eta[\beta_\eta, \beta_\phi](p) &= 2 \frac{\delta W_2[\beta_\eta, \beta_\phi]}{\delta \beta_\eta(p)}, \\ \Sigma_\phi[\beta_\eta, \beta_\phi](p) &= \frac{2}{N-1} \frac{\delta W_2[\beta_\eta, \beta_\phi]}{\delta \phi_\eta(p)}. \end{aligned} \quad (14)$$

Here, the simple relation $(\Sigma_\phi)_{ab} = \delta_{ab} \Sigma_\phi = 2 \frac{\delta W_2}{\delta (\beta_\phi)_{ab}} = \delta_{ab} \frac{2}{N-1} \frac{\delta W_2}{\delta \beta_\phi}$ was taken into account.

At sufficiently high temperature the symmetry is restored. This means that the value of the condensate is zero, $v = 0$, and the masses of the Higgs and the Goldstone fields are equal, $M_\eta = M_\phi$. Then the SD-equations (13) reduce to one equation, Eq. (7). At low temperature, the symmetry is broken and v is non zero. The masses are different and we have to consider two equations, Eqs. (13). Then, the free energy is the function of the condensate v . It has a minimum at $v > 0$ which can be seen already on the tree level. It may have more extrema. In that case due to the continuity of the free energy as a function of v an additional extremum for $v > 0$ must be a maximum indicating a first order phase transition.

Following [14], we consider the free energy in its extrema. We take the derivative of W with respect to the condensate v^2 ,

$$\frac{d}{dv^2} W_2[\beta_\eta, \beta_\phi] = \frac{m^2}{2} - \frac{\lambda}{2N} v^2 - \frac{3\lambda}{2N} \text{Tr} \beta_\eta - \frac{\lambda(N-1)}{2N} \text{Tr} \beta_\phi + \frac{\partial W_2[\beta_\eta, \beta_\phi]}{\partial v^2}. \quad (15)$$

In general, in this expression there are contributions proportional to $\partial \beta_\eta / \partial v^2$ and $\partial \beta_\phi / \partial v^2$. But they vanish by means of the SD-equations (13). In Eq. (15), $\frac{\partial W_2}{\partial v^2}$ denotes the derivative with respect to the explicit dependence on v entering through the vertex factors.

Demanding now the derivative given by Eq. (15) to vanish,

$$\frac{dW_2[\beta_\eta, \beta_\phi]}{dv^2} = 0, \quad (16)$$

we obtain the following equation,

$$\frac{\lambda}{N}v^2 = m^2 - 3\frac{\lambda}{N}\text{Tr}\beta_\eta - \frac{\lambda(N-1)}{N}\text{Tr}\beta_\phi + 2\frac{\partial W_2}{\partial v^2}, \quad (17)$$

which has to be considered together with the SD-equations (13).

In order to proceed it is necessary to make approximations. First of all, we put the momentum p in the SD-equations equal to zero, $p = 0$, that is, we turn to the corresponding gap equations. This is reasonable because we are interested in the infrared behavior and the gap in the spectrum is the decisive quantity. So we make the ansatz

$$\begin{aligned} \beta_\eta &= p^2 + M_\eta^2 \\ \beta_\phi &= p^2 + M_\phi^2 \end{aligned} \quad (18)$$

for the propagators and consider the SD equations (13) at $p = 0$. The assumption connected with this approximation is that the ultraviolet behavior of the propagator is mostly the same for the full solution and for (18), that the behavior for mediate momenta is not essential and that the important information is contained in the gap, i.e., in M_η and in M_ϕ . We note that in the super daisy approximation the corresponding contribution to Σ is independent of p and the approximation (18) becomes an exact relation.

The next approximation concerns the functional W_2 . Here, we restrict ourselves to graphs with at most two insertions of the trilinear vertex. In analytic notation we have

$$W_2[\beta_\eta, \beta_\phi] = W_2^{\text{SD}} + D + v^2\Gamma + O(v^4). \quad (19)$$

Contributions proportional to v^4 and higher powers of v^2 are dropped. Furthermore, we wrote down explicitly the lowest graphs, i.e., the graphs with one vertex, and introduced the notation D for the remaining ones. By construction, the graphs in D do not contain v -dependent vertices and have at least two vertices. The graphs with one vertex are

$$\begin{aligned} W_2^{\text{SD}} &= \frac{1}{8} \text{---} \text{---} \text{---} + \frac{1}{4} \text{---} \text{---} \text{---} + \frac{1}{4} \text{---} \text{---} \text{---} \\ &= -\frac{3\lambda}{4N}(\Sigma_\eta^{(0)})^2 - \frac{\lambda N - 1}{2N}\Sigma_\eta^{(0)}\Sigma_\phi^{(0)} - \frac{\lambda N^2 - 1}{4N}(\Sigma_\phi^{(0)})^2, \end{aligned} \quad (20)$$

where the solid line is the Higgs field propagator, β_η , and the broken line is the Goldstone one, β_ϕ . Taken as the approximation to W_2 these graphs generate all super daisy graphs. The vertex factors are adduced in the Appendix, Table 2. In W_2^{SD} Eq. (20) we introduced the notations

$$\begin{aligned}\Sigma_\eta^{(0)} &= \text{Tr}\beta_\eta = \text{---}\bigcirc\text{---} , \\ \Sigma_\phi^{(0)} &= \text{Tr}\beta_\phi = \text{- - -}\bigcirc\text{- - -} .\end{aligned}\quad (21)$$

Now, let us rewrite the gap equations in this approximation. In the restored phase, we have to put $v = 0$ and to take the corresponding functional derivatives. We obtain

$$\begin{aligned}M_\eta^2 &= -m^2 + \frac{3\lambda}{N}\Sigma_\eta^{(0)} + \lambda\frac{N-1}{N}\Sigma_\phi^{(0)} - 2\frac{\delta D}{\delta\beta_\eta}, \\ M_\phi^2 &= -m^2 + \frac{\lambda}{N}\Sigma_\eta^{(0)} + \lambda\frac{N+1}{N}\Sigma_\phi^{(0)} - \frac{2}{N-1}\frac{\delta D}{\delta\beta_\phi}.\end{aligned}\quad (22)$$

Taking into account that $\frac{\delta D}{\delta\beta_\eta} = \frac{1}{N-1}\frac{\delta D}{\delta\beta_\phi}$ holds at $M_\eta = M_\phi$ the two equations become equal for symmetry reasons and we are left with one equation for the mass in the restored phase which we denote as M_r .

In the broken phase, in the extremum of the free energy the condensate is given by Eq. (17). First, using the approximation (19) we rewrite the gap equations (13) as follows

$$M_\eta^2 = -m^2 + \frac{3\lambda}{N}v^2 + \frac{3\lambda}{N}\Sigma_\eta^{(0)} \quad (23)$$

$$+ \lambda\frac{N-1}{N}\Sigma_\phi^{(0)} - 2v^2\frac{\delta\Gamma}{\delta\beta_\eta} - 2\frac{\delta D}{\delta\beta_\eta}, \quad (24)$$

$$M_\phi^2 = -m^2 + \frac{\lambda}{N}v^2 + \frac{\lambda}{N}\Sigma_\eta^{(0)} \quad (25)$$

$$+ \lambda\frac{N+1}{N}\Sigma_\phi^{(0)} - v^2\frac{2}{N-1}\frac{\delta\Gamma}{\delta\beta_\eta} - \frac{2}{N-1}\frac{\delta D}{\delta\beta_\phi}. \quad (26)$$

The equation (17) resulting from the condition of the extremum takes the form

$$\frac{\lambda v^2}{N} = m^2 - \frac{3\lambda}{N}\Sigma_\eta^{(0)} - \lambda\frac{N-1}{N}\Sigma_\phi^{(0)} + 2\Gamma. \quad (27)$$

Now, by using Eq. (27) we rewrite the first gap equation, Eq.(23), in the form

$$M_\eta^2 = 2\left(1 - \frac{N}{\lambda}\frac{\delta\Gamma}{\delta\beta_\eta}\right)\left(m^2 - \frac{3\lambda}{N}\Sigma_\eta^{(0)} - \lambda\frac{N-1}{N}\Sigma_\phi^{(0)} + 2\Gamma\right), \quad (28)$$

where we took the relation $\Gamma = \frac{\delta D}{\delta \beta_\eta}$ into account. Then, by means of Eq. (23), we rewrite Eq. (27) as

$$\frac{\lambda}{N}v^2 = \left(1 - \frac{N}{\lambda} \frac{\delta \Gamma}{\delta \beta_\eta}\right)^{-1} \frac{M_\eta^2}{2}. \quad (29)$$

The second gap equation can be rewritten in a similar way. First we insert v from Eq. (17) in its first appearance and from Eq. (29) in its second one. We obtain finally

$$M_\phi^2 = \frac{2\lambda}{N} \left(\Sigma_\phi^{(0)} - \Sigma_\eta^{(0)}\right) - \frac{M_\eta^2}{N-1} \frac{\frac{\delta \Gamma}{\delta \beta_\phi}}{\frac{\lambda}{N} - \frac{\delta \Gamma}{\delta \beta_\eta}} + 2 \left(\Gamma - \frac{1}{N-1} \frac{\delta D}{\delta \beta_\phi}\right). \quad (30)$$

In this way all necessary general formulas are collected. In the next sections we will proceed with more specific approximations.

3 Super daisy approximation (SDA)

The super daisy approximation (sometimes the corresponding diagrams are called also cactus or foam diagrams) is the result of summing up all graphs containing lines closed up over one vertex. It is known that this resummation is equivalent to take in the functional W_2 , Eq. (9), the contribution of W_2^{SD} , (20), only. So, we have to put in the formulas given in the preceding section $\Gamma = D = 0$.

First, we write down the functional W , Eq. (12), in the chosen approximation. To that end we rewrite the contributions like $\text{Tr} \Delta_\eta^{-1} \beta_\eta$ by using the SD equations (13) and $\Sigma_\eta^{(0)}$ resp. $\Sigma_\eta^{(0)}$ in the right hand sides. Multiplying by $\beta_\eta(p)$ resp. $\beta_\phi(p)$ and taking the trace, by means of Eq. (21) we have

$$\begin{aligned} \text{Tr} \Delta_\eta^{-1} \beta_\eta(p) &= \left(\Sigma_\eta^{(0)}\right)^2 + c, \\ \text{Tr} \Delta_\phi^{-1} \beta_\phi(p) &= \left(\Sigma_\phi^{(0)}\right)^2 + c, \end{aligned}$$

where c is an irrelevant constant. Taking into account these relations we rewrite W as

$$W(v^2, M_\eta, M_\phi) = \frac{m^2}{2}v^2 - \frac{\lambda}{N}v^4 + \frac{1}{2}\text{Tr} \ln \beta_\eta + \frac{N-1}{2}\text{Tr} \ln \beta_\phi - W_2^{\text{SD}} \quad (31)$$

with W_2^{SD} given by Eq. (20). Here we explicitly denoted the arguments W depends on.

Now we turn to the gap equations. In the restored phase, we have $v = 0$ and the masses are equal, $M_\eta = M_\phi \equiv M_r$. There is only one equation following from Eqs. (22). Now it reads

$$M_r^2 = -m^2 + \lambda \frac{N+2}{N} \Sigma^{(0)}, \quad (32)$$

where in $\Sigma^{(0)}$ the propagator $\beta = 1/(p^2 + M_r^2)$ has to be inserted, similar to Eqs. (21). The corresponding value of W is $W(0, M_r, M_r)$.

In the broken phase, we first note Eq. (29) which takes the form

$$\frac{\lambda}{N}v^2 = \frac{1}{2}M_\eta^2. \quad (33)$$

The gap equations (28), (30) turn into

$$\begin{aligned} M_\eta^2 &= 2 \left(m^2 - \frac{3\lambda}{N}\Sigma_\eta^{(0)} - \lambda \frac{N-1}{N}\Sigma_\phi^{(0)} \right), \\ M_\phi^2 &= \frac{2\lambda}{N} (\Sigma_\phi^{(0)} - \Sigma_\eta^{(0)}). \end{aligned} \quad (34)$$

Finally, we take the high temperature expansion for the functions entering. They are well known and we use them in the form given in our previous papers [16, 14]:

$$\begin{aligned} V_1(M) \equiv -\frac{1}{2}\text{Tr} \ln \beta &= \frac{-\pi^2 T^4}{90} + \frac{M^2 T^2}{24} - \frac{M^3 T}{12\pi} + \dots, \\ \Sigma^{(0)} &= \frac{T^2}{12} - \frac{MT}{4\pi} + \dots, \end{aligned} \quad (35)$$

where the corresponding masses M_r , M_η or M_ϕ have to be inserted. In Eqs. (35), the dots denote contributions suppressed by higher powers of M/T .

In this approximation the gap equations read, in the restored phase,

$$M_r^2 = -m^2 + \frac{\lambda(N+2)T^2}{12N} - 2M_r \frac{\lambda(N+2)T}{8\pi N}, \quad (36)$$

and in the broken phase,

$$\begin{aligned} M_\eta^2 &= 2m^2 - \frac{\lambda(N+2)T^2}{6N} + 2M_\eta \frac{3\lambda T}{4\pi N} + M_\phi \frac{\lambda(N-1)T}{2\pi N}, \\ M_\phi^2 &= \frac{\lambda T}{2\pi N} (M_\eta - M_\phi). \end{aligned} \quad (37)$$

In the restored phase, Eq. (36) can be solved simply with the result

$$M_r = -\frac{\lambda(N+2)T}{8\pi N} + \sqrt{\left(\frac{\lambda(N+2)T}{8\pi N}\right)^2 - m^2 + \frac{\lambda(N+2)T^2}{12N}}. \quad (38)$$

We observe that it has a single solution for positive mass as long as $T > T_-$, where

$$T_- = \sqrt{\frac{12N}{\lambda(N+2)}}m \quad (39)$$

is the lower spinodal temperature.

In the broken phase, the two gap equations (37) form a system of algebraic equations. While in the one component case there had been one equation of second order (a quadratic equation like Eq. (36) in the restored phase), here the order is higher because there are two coupled equations. We proceed as follows. The second equation can be solved with respect to M_ϕ ,

$$M_\phi(M_\eta) = -\frac{\lambda T}{4\pi N} + \sqrt{\left(\frac{\lambda T}{4\pi N}\right)^2 + \frac{\lambda T}{2\pi N}M_\eta}. \quad (40)$$

This is a unique solution $M_\phi(M_\eta)$ for all T . Note the special value $M_\phi(0) = 0$ independent of T .

Now we insert $M_\phi(M_\eta)$ from (40) into the first equation in formula (37),

$$M_\eta^2 = 2m^2 - \frac{\lambda(N+2)T^2}{6N} + 2M_\eta \frac{3\lambda T}{4\pi N} + \frac{\lambda(N-1)T}{2\pi N}M_\phi(M_\eta). \quad (41)$$

This equation can be written down as a fourth order algebraic equation. But for a moment let us rewrite it formally by solving as a quadratic equation for M_η keeping $M_\phi(M_\eta)$,

$$M_\eta = \frac{3\lambda T}{4\pi N} \pm \sqrt{\left(\frac{3\lambda T}{4\pi N}\right)^2 + 2m^2 - \frac{\lambda(N+2)T^2}{6N} + \frac{\lambda(N-1)T}{2\pi N}M_\phi(M_\eta)}. \quad (42)$$

For $T = 0$ we have a solution for the upper sign which is clearly the mass in the minimum of the free energy. Hence the solution with the lower sign describes a maximum. This mass vanishes for $T = T_-$ (taking into account Eqs. (39) and (40)).

Eq. (41) has an explicit solution, which is, however, too large to be displayed here. It can be easily plotted and is shown in Figure 1. We have chosen $\lambda = 1$ in order to make the details near the phase transition better visible. But we can obtain the basic properties of this solution in the following way. Assume we plot the rhs. versus lhs. of Eq. (41). We observe that for small T there is one solution. At $T = T_-$ a second solution appears and at some temperature T_+ both solutions merge and disappear. So T_+ has to be interpreted as the upper spinodal temperature. In this way we observe a first order phase transition. Once we have an algebraic solution of the gap equations, we can give an algebraic expression for T_+ . Again, it is too complicated to be displayed. However, for small λ , T_+ can be expressed as

$$\frac{T_+}{T_-} = 1 + t_N \lambda + O(\lambda^2), \quad (43)$$

where the numbers t_N are algebraic expressions in N . Some numerical values are given in Table 1. For $N = 1$ we reobtain with $t_1 = \frac{9}{16\pi^2}$ the known result from

N	0	1	2	3	4	5
t_N	0.0569932	0.029511	0.0203949	0.0158314	0.0130797	0.0112318

Table 1: Some numerical values of the coefficients t_N in Eq. (43)

the one component case in [14]. In the limit of large N we obtain

$$t_N \sim \frac{9\lambda}{16\pi^2} \frac{1}{(2N)^{\frac{2}{3}}} \quad (44)$$

which shows that the phase transition becomes second order for large N .

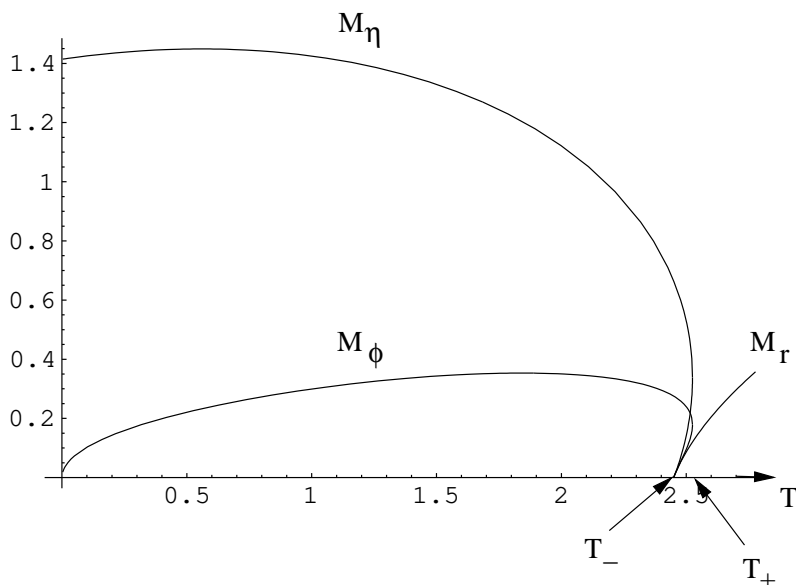


Figure 1: The masses M_η , M_ϕ and M_r as functions of the temperature T for $\lambda = 1$, $N = 2$. The upper parts of the curves for M_η and M_ϕ show the corresponding masses in the minimum of the free energy, the lower parts show the masses in the maximum.

Now, having solved the gap equation, we consider the functional W . Let W_b be its value in the minimum (broken phase), given by Eq. (31) with the masses inserted from the solutions discussed above and the condensate v from Eq. (33). Let $W_r = W(0, M_r, M_r)$ be the corresponding value in the restored phase. Again, the analytic expressions are too large to be displayed. So, we restrict ourselves to some numerical values. For example, for $\lambda = 1$ and $N = 2$ we have $T_- = 2.44949$ and $T_+ = 2.52514$. In $T = T_-$ we have $W_b = -8.15081$ and $W_r = -8.14568$ (note that the free energy differs in sign from W , see Eq. (3)). In $T = T_+$ the corresponding values are $W_b = -8.15081$ and $W_r = -9.1671$. In Figure 2 we plotted $F = -\Delta W/T$ as function of the temperature in the region of the phase transition, i.e., for $T_- \leq T \leq T_+$. The temperature T_c of the phase transition follows from $\Delta W \equiv W_b - W_r = 0$ to be $T_c = 7.767$.

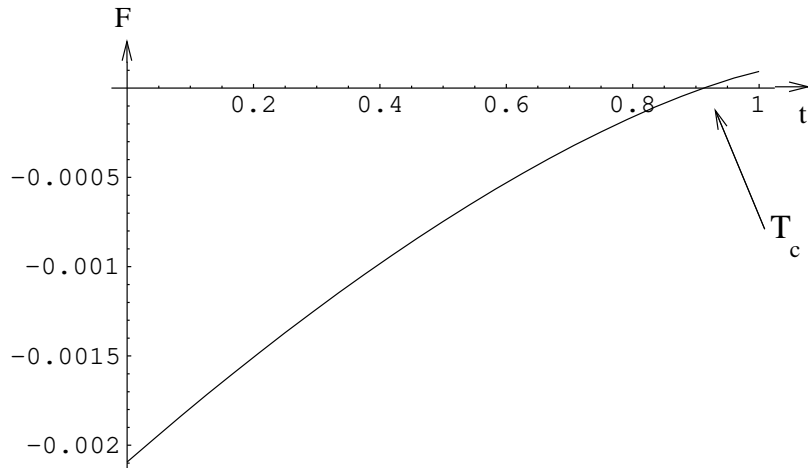


Figure 2: The free energy F as function of t parameterizing by means of $T = T_- + t(T_+ - T_-)$ the temperature in between T_- and T_+ .

4 Beyond the super daisy approximation (BSDA)

In this section we investigate the phase transition beyond the SDA. In the chosen approach of representing the free energy by the 2PI functional W_2 an approximation is given by choosing an approximation for W_2 . While we in the preceding section took the 3 graphs shown in Eq. (20) we include now all graphs consisting of rings (necklaces) of doubled lines. These are shown in Eq. (71) in the Appendix in generic form. In the unbroken phase where all fields have the same mass and there are no triple vertices, these represent all graphs where the summation over the internal indices is to be understood. In the broken phase we have to consider both kinds of fields, η and ϕ , and the triple vertices. The number of the corresponding graphs becomes larger. The motivation for this choice is that in the unbroken phase these are all graphs in the next-to-next-to-leading order for large N . The leading order is given by the tree approximation, the next-to-leading order by the SDA in the preceding section.

As the expressions in this approximation beyond SDA are quite involved we are forced to make further approximations.

The aim of the present section is to find out whether the results found in the SDA are stable with respect in the next order. For this reason we restrict ourselves to the consideration of the SD equations in the broken phase, Eqs. (23) and (25), which we rewrite here in the form

$$\begin{aligned}
 M_\eta^2 &= 2\tilde{\Gamma} \left(m^2 - \frac{3\lambda}{N} \Sigma_\eta^{(0)} - \lambda \frac{N-1}{N} \Sigma_\phi^{(0)} + 2\Gamma \right), \\
 M_\phi^2 &= \frac{2\lambda}{N} \left(\Sigma_\phi^{(0)} - \Sigma_\eta^{(0)} \right) - gM_\eta^2 + f,
 \end{aligned} \tag{45}$$

where the notations

$$\begin{aligned}
\tilde{\Gamma} &= 1 - \frac{N}{\lambda} \frac{\delta\Gamma}{\delta\beta_\eta(0)}, \\
g &= \frac{N}{\lambda(N-1)2\tilde{\Gamma}} \frac{\delta\Gamma}{\delta\beta_\phi(0)}, \\
f &= 2 \left(\frac{\delta D}{\delta\beta_\eta(0)} - \frac{1}{N-1} \frac{\delta D}{\delta\beta_\phi(0)} \right)
\end{aligned} \tag{46}$$

have been introduced. The functions $\frac{\delta D}{\delta\beta_\phi(0)}$ and $\Gamma = \frac{\delta D}{\delta\beta_\eta(0)}$ entering here, consist of the graphs shown in the Appendix, Eqs. (60) and (72). The corresponding analytic expressions are given by Eqs. (63) and (79). Now we need to take the high- T approximation of these functions. For this reason we consider their generic form. Consider, for example, the fragment

$$\text{Tr}_q \beta_\phi(q) a A = \text{Tr}_q \beta_\phi(q) \frac{\left(\frac{-3\lambda}{N} \Sigma_\eta^{(1)}(q) \right)^2}{1 + \frac{3\lambda}{N} \Sigma_\eta^{(1)}(q)},$$

entering Eq. (65). Note, that the external momentum is zero as we consider the gap equations. Now we approximate the function A , Eq. (66), entering here, by a constant, namely its value at zero momentum, $A \rightarrow A|_{q=0}$. As A is a dimensionless function which does not change its sign, in the remaining integral the behavior of the integrand is changed only slightly. Then we take the high- T approximation. The quantities a , b and c can be calculated in a standard way, see e.g. $\Sigma_1(p)$ in Eq. (57) in [14],

$$\begin{aligned}
a &= \frac{-3\lambda T}{8\pi N} \frac{1}{M_\eta} + \dots, \\
b &= \frac{-3\lambda T}{8\pi N} \frac{N+1}{3} \frac{1}{M_\phi} + \dots, \\
c &= \frac{-3\lambda T}{8\pi N} \frac{2}{3} \frac{2}{M_\eta + M_\phi} + \dots,
\end{aligned} \tag{47}$$

where the dots indicate contributions suppressed by powers of M/T . The remaining expressions correspond to graphs of the basket ball type. They have been calculated frequently. In the high- T approximation they read

$$\begin{aligned}
\text{Tr}_q \beta_\eta(q) a &= \text{Tr}_q \beta_\eta(q) \frac{-3\lambda}{N} \Sigma_\eta^{(1)}(q) = \frac{-3\lambda T^2}{32\pi^2 N} \gamma_1 + \dots \\
\text{Tr}_q \beta_\eta(q) b &= \text{Tr}_q \beta_\eta(q) \frac{-3\lambda}{N} \frac{N+1}{3} \Sigma_\phi^{(1)}(q) = \frac{-3\lambda T^2}{32\pi^2 N} \frac{N+1}{3} \gamma_2 + \dots \\
\text{Tr}_q \beta_\eta(q) c &= \text{Tr}_q \beta_\eta(q) \frac{-2\lambda}{N} \Sigma_{\eta\phi}^{(1)}(q) = \frac{-3\lambda T^2}{32\pi^2 N} \frac{2}{3} \gamma_4 + \dots
\end{aligned}$$

$$\begin{aligned}
\text{Tr}_q \beta_\phi(q)a &= \text{Tr}_q \beta_\phi(q) \frac{-3\lambda}{N} \Sigma_\phi^{(1)}(q) = \frac{-3\lambda T^2}{32\pi^2 N} \gamma_4 + \dots \\
\text{Tr}_q \beta_\phi(q)b &= \text{Tr}_q \beta_\phi(q) \frac{-3\lambda}{N} \frac{N+1}{3} \Sigma_\phi^{(1)}(q) = \frac{-3\lambda T^2}{32\pi^2 N} \frac{N+1}{3} \gamma_3 + \dots \\
\text{Tr}_q \beta_\phi(q)c &= \text{Tr}_q \beta_\phi(q) \frac{-2\lambda}{N} \Sigma_{\eta\phi}^{(1)}(q) = \frac{-3\lambda T^2}{32\pi^2 N} \frac{2}{3} \gamma_2 + \dots
\end{aligned} \tag{48}$$

with

$$\begin{aligned}
\gamma_1 &= 1 - 2 \ln \frac{3M_\eta}{\mu}, \\
\gamma_2 &= 1 - 2 \ln \frac{M_\eta + 2M_\phi}{\mu}, \\
\gamma_3 &= 1 - 2 \ln \frac{3M_\phi}{\mu}, \\
\gamma_4 &= 1 - 2 \ln \frac{2M_\eta + M_\phi}{\mu},
\end{aligned} \tag{49}$$

where μ is a normalization constant. Again, by the dots higher orders in M/T are indicated.

In this way, we have analytic expressions for the functions entering the gap equations (45) which can be written as

$$\begin{aligned}
\Gamma &= \frac{-3\lambda^2 T^2}{32\pi^2 N^2} \left\{ \gamma_1(1+3A) + (N+1)\gamma_2(\epsilon+B) \right. \\
&\quad \left. + 3 \frac{\gamma_1}{a} \frac{(2+a+B)AB}{1-AB} + \frac{2}{3}(N-1)\gamma_2 \frac{c}{1-c} \right\},
\end{aligned} \tag{50}$$

$$\begin{aligned}
\frac{\delta\Gamma}{\delta\beta_\eta(0)} &= \frac{-\lambda}{N} \left\{ (1+2a\partial_a) \left[a(1+3A) + 3 \frac{(2+a+B)AB}{1-AB} \right] \right. \\
&\quad \left. + 2 \frac{N-1}{N+1} b \partial_c \frac{c^2}{1-c} \right\}
\end{aligned} \tag{51}$$

and

$$\begin{aligned}
\frac{\delta D}{\delta\beta_\phi(0)} &= \frac{-3\lambda^2 T^2}{32\pi^2 N^2} \left\{ \frac{(N+1)^2}{3} \gamma_3 \left[\frac{1}{3} + \frac{b}{1-b} + 2 \frac{N-2}{N+1} \left(\frac{1}{3} + \frac{2}{N+1-2b} \right) \right] \right. \\
&\quad + (N-1) \left[\frac{1+A}{3} \gamma_4 + \frac{\gamma_4}{3\epsilon a} \frac{(2+\epsilon A + \frac{1}{\epsilon} B) AB}{1-AB} \right] \\
&\quad \left. + (N-1) \frac{2\gamma_2}{3} \frac{c}{1-c} \right\}
\end{aligned} \tag{52}$$

with a , b and c given by Eqs. (47), for the remaining notations see the Appendix.

The functions $\Sigma^{(0)}$ entering the gap equations have been given for high T in the preceding section by Eqs. (34). Here, in order to be consistent with (48), we include one more term into the expansion, i.e., we take

$$\Sigma^{(0)} = \frac{T^2}{12} - \frac{MT}{4\pi} + \frac{M^2 L_n + 2m^2}{16\pi^2} + \dots \quad (53)$$

with the notation

$$L_n = \ln \frac{(4\pi T)^2}{2m^2} - 2\gamma, \quad (54)$$

where γ is Euler's constant gamma.

Inserting these approximations we rewrite the gap equations (45) in the form

$$\begin{aligned} M_\eta^2 &= 2h \left(m^2 \delta_1 - \frac{\lambda T^2}{4N} \delta_\gamma + D_\phi + M_\eta \frac{3\lambda T}{4\pi N} \right), \\ M_\phi^2 &= \frac{\lambda T}{2\pi N} \frac{-M_\phi^2}{M - \eta + M_\phi} + \frac{\lambda L_n}{8\pi^2 N_g} M_\eta^2 + f \end{aligned} \quad (55)$$

with

$$\begin{aligned} D_\phi &= \frac{\lambda(N-1)T}{4\pi N} M_\phi - \frac{\lambda(N-1)L_n}{16\pi^2 N} M_\phi^2, \\ h &= \frac{\tilde{\Gamma}}{1 + 2\tilde{\Gamma} \frac{3\lambda L_n}{16\pi^2 N}}, \\ \delta_1 &= 1 - \frac{3\lambda}{8\pi^2 N} \frac{N+2}{3}, \\ \delta_\gamma &= \frac{N+2}{N} - \frac{3\lambda}{4\pi N} \left(\frac{N+2}{N} - 2 \ln \frac{3M_\eta}{\mu} - s \ln \frac{M_\eta + 2M_\phi}{\mu} \right). \end{aligned} \quad (56)$$


The quantity D_ϕ , entering the first gap equation, depends on m_ϕ which must be found from the second equation as a function of m_η .

Now, we investigate qualitatively these equations and plot both sides in one plot. The lhs. is simply part of a parabola. The rhs. have a more complicated behavior. For large M_η resp. M_ϕ they remain smaller than the lhs because of additional factors λ in front. For small M_η in the rhs. of the first equation we note

$$\begin{aligned} h &= \frac{8\pi^2 N}{3\lambda L_n} + O(M_\eta), \\ \delta_\gamma &= \frac{3\lambda}{\pi N} \ln \frac{1}{M_\eta} + O(M_\eta), \end{aligned} \quad (57)$$

so that it takes negative values for small M_η .

It is interesting to compare with the expansion of these quantities for small λ . This corresponds to take the first graph out of the infinite sequence (71). In

the SD equation this means to take the graph  in addition to $\Sigma^{(0)}$, Eq. (21), in the self energy part. As an approximation, this is in between SDA and BSAD and does not include the effect from summing up the infinite chain of doubled lines. We call this perturbative approximation beyond the super daisy approximation (pBSDA). So, in pBSDA it holds

$$h = 1 + \dots \quad (58)$$

$$\delta_\gamma = \frac{N+2}{3} \left(1 - \frac{3\lambda}{4\pi N}\right) + \frac{3\lambda}{2\pi N} \left(\ln \frac{3M_\eta}{\mu} + \frac{N-1}{3} \ln \frac{M_\eta + 2M_\phi}{\mu}\right) + \dots$$

Note, that δ_γ takes for sufficiently small M_η negative values in opposite to (57).

The rhs. of the first equation is shown in Figure 3 in both approximations for a temperature near the phase transition. The curve corresponding to the pBSDA starts from some finite value at $M_\eta = 0$. For small temperature ($T < T_-$ where T_- has to be taken in the given approximation) it starts from positive values and has one intersection with the lhs. corresponding to one extremum only of the free energy. In opposite, for $T > T_-$ it starts from negative values and has two intersections indicating the existence of a maximum. For larger T , the curve lowers until its two intersections with the lhs. merge at the corresponding T_+ . This case is just shown in the figure. This is qualitatively the same behavior as in the SDA case. Now consider the BSDA case. Here, due to the logarithmic behavior in Eq. (57), the curve starts for any temperature from negative values and we have a second extremum (which must correspond to a maximum) for any temperature $T < T_+$. So, formally, we observe $T_- = 0$. However, these negative values to be realized the logarithm must be large, $\ln M_\eta \sim -\frac{\pi^2 N}{3\lambda}$. This is the only qualitative change coming in from the BSDA resummation and it is of extreme smallness. In general, it is a quite remarkable fact that the resummation results in a denominator (combinations $1 - a$, $1 - b$, $1 - c$ and $1 - AB$) which does not have a zero in the region we are interested in. Comparing the curves in Figure 3, we see that the quantitative difference between the different approximation is quite large.

Let us now consider the second equation. It is shown in Figure 4. As one can see, in any case in both approximations it has a solution which is similar to the simple solution of the second equation in the SDA case, Eq. (40). However, for some value s of the parameters, there may be three solutions as seen from the figure. This is the substructure of the phase transition which deserves further investigation.

Having clarified the general behavior of the solutions of the gap equations, one can start a numerical investigation. Results are shown in backing the qualitative similarity to the SDA. A numerical solution in the BSDA case is shown in Figure 4. It shows qualitatively the same behavior as in the SDA case which is shown in the lower plot in Figure 4 for the same value of $\lambda = 0.1$. We note that the solution in the restored phase starts in the BSAD case at considerably smaller T .

In fact it starts from $T = 0$ but there it is exponentially small.

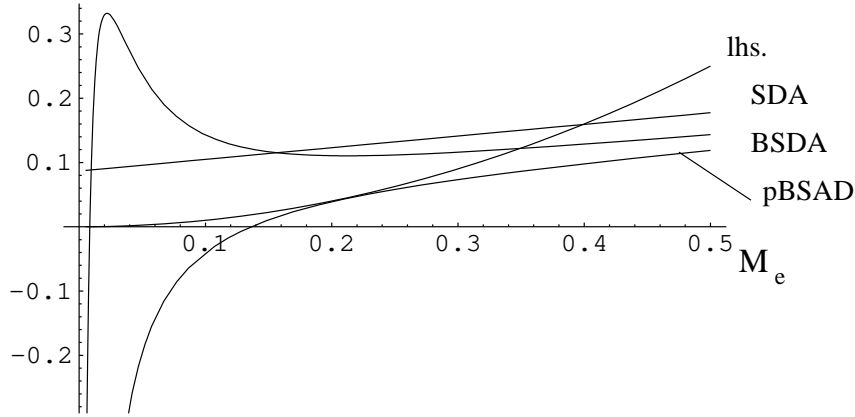


Figure 3: The lhs. and the rhs. of the first gap equation, (55), for different approximations as function of the mass M_η for $\lambda = 0.1$, $T = 7.7$, $M_\phi = 0.2$.

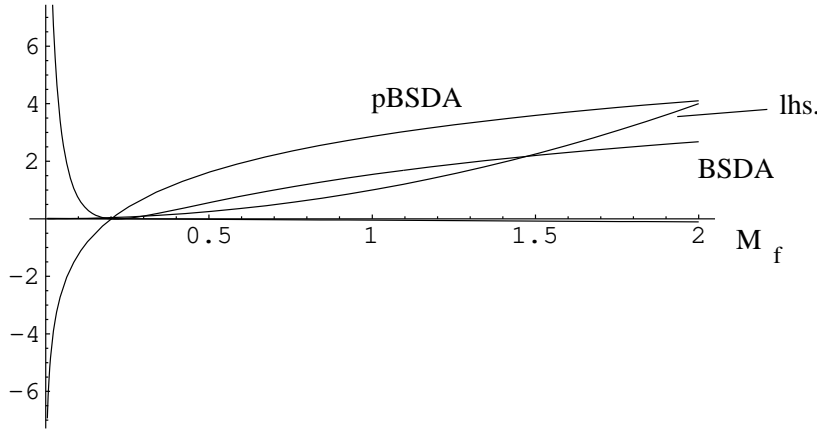


Figure 4: The lhs. and the rhs. of the second gap equation, (55), for different approximations as function of the mass M_ϕ for $\lambda = 0.1$, $T = 7.7$, $M_\eta = 0.2$.

5 Conclusions

We investigated the phase transition in the $O(N)$ -model by perturbative methods. As technical tools we used the second Legendre transform and the method of considering the gap equations in the extrema of the free energy. The latter simplifies the expressions considerably and allows for more explicit results.

We considered two stages of approximation. We started with the super daisy approximation. Here, for small coupling λ , which is by means of Eq. (39),

equivalent to high temperature, we obtained clearly a first order phase transition. This generalizes the corresponding results obtained in the one component case found in [14]. The masses of the Higgs and Goldstone particles in the broken phase and the mass of the field in the restored phase are shown in Figure 1. The corresponding free energy is shown in Figure 2. It should be noticed that the first order character of the phase transition is extremely weak. As can be seen from Figure 2, the change in the free energy between T_c and T_- is numerically small as compared to the mass scale which is set to unit in that figure. Also, the difference between the two spinodal temperatures, Eq. (43), is of order λ . So, to leading order in λ the transition is of second order and the first order character is a next-to-leading effect in λ . For large N , from Eq. (44) it follows that the transition becomes second order.

In order to check the reliability of the results obtained in SDA we calculated in Section 4, beyond the SDA, the next class of graphs (BSAD). In the unbroken phase these are all graphs in the next-to-next-to-leading order in $1/N$. They are given by Eq. (71) and their dependence on N is taken into account completely (not only for large N). These graphs can be characterised as chains of doubled lines. The summation of the infinite set of these graphs is performed for the quantities entering the gap equations. Then the resulting quantities have been calculated approximatively for high temperature where in essence besides the leading contribution only the logarithmic terms, Eq. (49), have been taken into account. As the remaining expressions are quite complicated, the gap equations have been solved numerically. An example for such a solution is shown in Figure 4. The general outcome is that the results obtained in SDA remain valid qualitatively. They are altered in details. For instance, there exists a maximum of the free energy for any $T < T_+$ so that formally we have $T_- = 0$. However, for small T this maximum is exponentially small (it is due to the logarithmic terms). Also, there appear additional solutions (M^* in Figure 4). In this way we confirmed in the N -component case the results found in [14] for the one component case stating that the results in SAD are qualitatively stable with respect to higher loops.

With these results obtained we are left with the difficult problem that all nonperturbative approaches (lattice calculations, flow equations, etc.) predict a second order character for the transition. In the absence of a small expansion parameter near the phase transition it was reasonable to believe that the origin of the discrepancy between the perturbative and non perturbative results is due to this fact. If this is the case, it is important to find out the type of diagrams responsible for the change of the type of the phase transition.

Now, we are going to comment some calculations where the second order phase transition has been determined. First we discuss the observation in Ref.[13] that the inclusion of a two-loop diagram beyond the super daisy resummation results in a second order phase transition. The diagram mentioned is the first one in a series depicted in Eq. (60) in the Appendix. Its exclusion does not change signifi-

cantly the structure of the gap equations and the solutions obtained if, of course, all other diagrams are taken into consideration. Hence, we conclude that this diagram does not change the type of the phase transition. In Ref.[17] the second order phase transition was observed when the renormalization group method at finite temperature has been applied. Results obtained in this way are difficult to compare with that found in the case of the standard renormalization at zero temperature adopted in the present paper. The point is that the renormalization at finite temperature replaces some resummations of a series of diagrams which remains unspecified basically.

In Refs.[12, 13] new non perturbative method of calculation of the effective potential at finite temperature - an auxillary field method - has been developed and a second order phase transition was observed for both the one- and N -component models. We left the detailed analysis of this method for other publication and here just mention that it seems to us not a self-consistent one because it delivers an imaginary part to the effective potential in its minima. This important point is crucial for any calculation scheme as a whole. Really, the minima of the effective potential describe physical vacua of a system. An imaginary part is signaling either the false vacuum or the inconsistency of the calculation procedure used. That is well known starting from the work by Dolan and Jackiw [18] who noted the necessity of resummations in order to have a real effective potential at finite temperature. The key point of the procedure in Refs.[12, 13] is to relate the total polarization operator and the one-loop effective potential. But it is difficult to achieve on some reasonable grounds because these entities are different parts of the effective action in the derivative expansion. Hence, it is difficult to estimate the correctness of the method, its stability with respect to some small deviations, etc. In our method of calculations the stability of the vacuum is automatically satisfied when the super daisy diagrams are resummed in the extrema of the free energy.

As we have seen, the SDA possesses a lot of attractive features. In particular, the results obtained in this way are qualitatively stable with respect to other resummations. So, it is reasonable to investigate in more detail its properties as well.

Appendix

In this appendix we calculate and sum up the bubble chain graphs appearing in the gap equations in sections 2 and 4. The corresponding well known Feynman rules are collected in Table 2. The vertex (ϕ^4) contains the symmetric tensor

$$V_{abcd} = \frac{1}{3} (\delta_{ab}\delta_{cd} + \delta_{ac}\delta_{bd} + \delta_{ad}\delta_{bc}). \quad (59)$$

The functional Γ introduced in (19) consists of all graphs with 2 triple vertices, (η^3) or ($\eta\phi^2$), i.e., of all graphs proportional to v^2 and having at least 2 vertices.

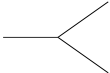
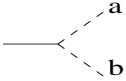
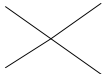
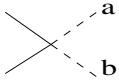
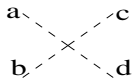
graphic element	corresponding field	propagator
	η	$\beta_\eta = (p^2 + M_\eta^2)^{-1}$
	ϕ_a	$\beta_\phi = (p^2 + M_\phi^2)^{-1}$
graphic element	vertex factor	notation
	$-\frac{6\lambda v}{N}$	(η^3)
	$-\frac{6\lambda v}{N}\delta_{ab}$	$(\eta\phi^2)$
	$-\frac{2\lambda}{N}$	(η^4)
	$-\frac{2\lambda}{N}\delta_{ab}$	$(\eta^2\phi^2)$
	$-\frac{6\lambda}{N}V_{abcd}$	(ϕ^4)

Table 2: The Feynman rules for the $O(N)$ -model

In the approximation made in Section 5 the graphical representation is

$$\begin{aligned}
v^2\Gamma &= \frac{1}{12} \text{ (circle with vertical line) } + \frac{1}{8} \text{ (teardrop shape) } + \frac{1}{16} \text{ (cylinder) } + \dots \\
&+ \frac{1}{4} \text{ (teardrop with dashed back) } + \frac{1}{8} \text{ (cylinder with dashed back) } + \frac{1}{8} \text{ (cylinder with dashed front) } + \dots \\
&+ \frac{1}{4} \text{ (circle with dashed vertical line) } + \frac{1}{8} \text{ (teardrop with dashed back) } + \frac{1}{16} \text{ (cylinder with dashed back) } + \dots \\
&+ \frac{1}{2} \text{ (teardrop with dashed back) } + \frac{1}{2} \text{ (cylinder with dashed back) } + \dots \quad (60)
\end{aligned}$$

These are all graphs forming rings (necklaces) of doubled lines (or bubble chains). We denote them by

$$\begin{aligned}
\Sigma_\eta^{(1)}(p) &= \text{Tr}_q \beta_\eta(p+q) \beta_\eta(q), \\
\Sigma_\phi^{(1)}(p) &= \text{Tr}_q \beta_\phi(p+q) \beta_\phi(q), \\
\Sigma_{\eta\phi}^{(1)}(p) &= \text{Tr}_q \beta_\eta(p+q) \beta_\phi(q). \quad (61)
\end{aligned}$$

The loop integration in the graphs (60) are all in the just defined functions $\Sigma^{(1)}$ except for one integration flowing through the single line. It is useful to introduce the following notations,

$$\begin{aligned}
a &\equiv \frac{-3\lambda}{N} \Sigma_\eta^{(1)}(p), \\
b &\equiv -\lambda \left(1 + \frac{1}{N}\right) \Sigma_\phi^{(1)}(p), \\
c &\equiv \frac{-2\lambda}{N} \Sigma_{\eta\phi}^{(1)}(p). \quad (62)
\end{aligned}$$

Here the vertex factors and the symmetry factor (1/2) for $\Sigma_\eta^{(1)}(p)$ and $\Sigma_\phi^{(1)}$ are included as well as the factors resulting from the summation over the internal indices $a, b, \dots = 1, 2, \dots, N-1$. For them we used

$$\sum \delta_{ab} \delta_{cd} = N-1 \equiv V_1,$$

and

$$\sum \delta_{ab} V_{aba_1 b_1} V_{a_1 b_1 a_2 b_2} \cdots V_{a_{n-1} b_{n-1} cd} \delta_{cd} = (N-1) \left(\frac{N+1}{3} \right)^{n-1} \equiv V_n.$$

In terms of these abbreviations, Γ can be written as

$$\Gamma = \frac{-6\lambda}{N} \text{Tr}_p \beta_\eta(p) \gamma_a - \frac{\lambda(N-1)}{N} \text{Tr}_p \beta_\phi(p) \gamma_b \quad (63)$$

with

$$\begin{aligned} \gamma_a &= \frac{a}{6} + \frac{1}{2}a^2 + \dots + \frac{1}{2}\epsilon b + \frac{1}{2}\epsilon b^2 + \dots + \epsilon ab + \epsilon a^2 b + \epsilon ab^2 + \dots \\ &\quad + \frac{1}{2}c^2 + \frac{1}{2}c^3 + \dots, \end{aligned} \quad (64)$$

$$\gamma_b = c^2 + c^3 + \dots, \quad (65)$$

where the notation $\epsilon \equiv \frac{N-1}{3(N+1)}$ has been introduced which appears as a factor in front of each sequence of symbols b .

The symmetry factors of the graphs result in factors $\frac{1}{2}$ for sequences of symbols which are symmetric under transposition. Non symmetric sequences like ab appear only once because ba describes the same graph. Now we pull out the symmetry factor $\frac{1}{2}$ and correct that for the non symmetric sequences by writing them twice, e.g., $ab + ba$ instead of ab .

In this way we are faced with the sum over all sequences of symbols a and b . As a symbolic notation for the subgraphs in Γ they have to be taken to be non commuting. After inserting the analytical expressions in momentum space representation, in fact they do commute. But first let us sum up these sequences.

We observe that for each sequence containing a single factor a , i.e. a fragment $\dots bab \dots$, there is a sequence containing $baab$ instead, $baaab$, etc. These sequences can be summed up partially,

$$\sum_{i=1}^{\infty} \dots b \underbrace{a \dots a}_i b \dots = \dots b A b \dots,$$

where the notation

$$A \equiv \frac{a}{1-a} \quad (66)$$

was introduced. With other words, multiple neighbored factors a appear after this partial resummation only within the combination A . An exception is the sequence consisting of one single a which is treated separately by writing $\frac{a}{3} = a - \frac{2a}{3}$. The same holds for the sequences of symbols b where in addition a factor ϵ has to be taken into account. The summation results in

$$\sum_{i=1}^{\infty} \dots a \epsilon \underbrace{b \dots b}_i a \dots = \dots a B a \dots$$

with

$$B \equiv \frac{\epsilon b}{1-b}. \quad (67)$$

After these resummations, γ_a , (64), takes the form

$$\gamma_a = \frac{1}{2} \left(-\frac{2a}{3} + A + B + A^2 + B^2 + AB + BA + \dots \right).$$

Now the sequence of A 's and B 's can be summed up and we arrive finally at

$$\gamma_a = \frac{1}{2} \left(-\frac{2a}{3} + \frac{A + B + 2AB}{1 - AB} \right). \quad (68)$$

The sequences containing c form a simple geometric series

$$\sum_{i=2}^{\infty} c^i = cC$$

and with the notation

$$C = \frac{c}{1-c}. \quad (69)$$

we obtain

$$\gamma_b = cC. \quad (70)$$

In this way, by means of Eqs. 68 and (70) we obtained the complete expression for the functional Γ , Eq. (63).

Next we have to consider the functional D appearing in W_2 , Eq. (19). It is the sum of all graphs containing only quartic vertices and at least 2 loops. Again, within the approximation made in Sect. 4, we restrict ourselves to the contributions consisting of rings of doubled lines. In the case where there is one field only the corresponding graphical representation is

$$\begin{aligned}
 D &= \frac{1}{48} \text{ (ring of 2 lines) } + \frac{1}{48} \text{ (ring of 3 lines) } + \frac{1}{128} \text{ (ring of 4 lines) } + \dots, \\
 &= \frac{1}{48} \text{ (ring of 2 lines) } + \sum_{n \geq 3} \frac{1}{2^n n} \text{ (ring of } n \text{ lines) }, \quad (71)
 \end{aligned}$$

which is the same as Eq. (9) in [14]. In the N -component case with unbroken symmetry the corresponding expression are essentially the same. For broken

symmetry they become more complicated. However, in the gap equations we need the derivatives $\delta D/\delta\beta_\eta(p)$ and $\delta D/\delta\beta_\phi(p)$ only. By means of the relation

$$\Gamma = \frac{\delta D}{\delta\beta_\eta(p)}$$

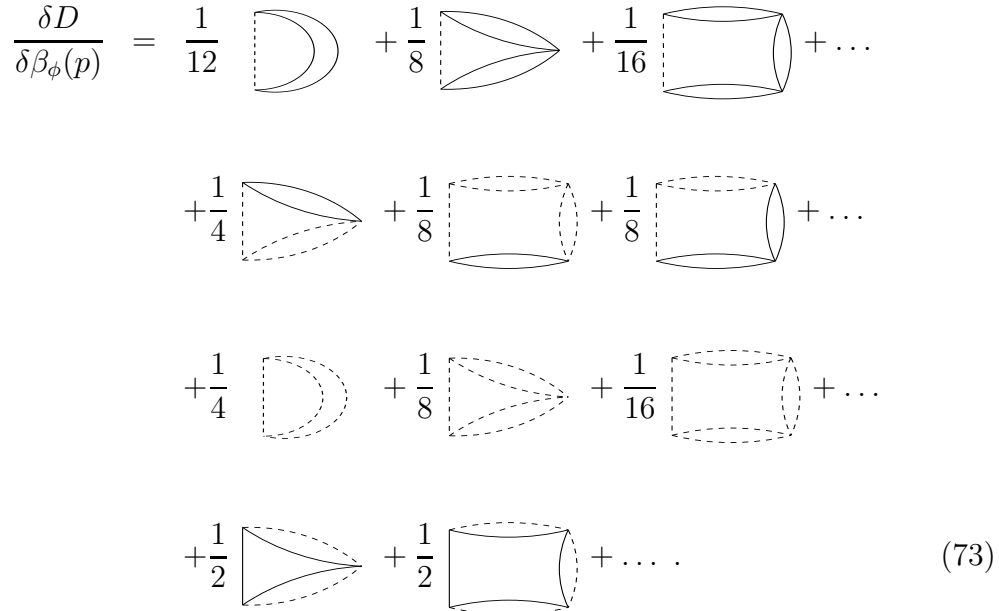
one of them is already calculated and we are left with $\delta D/\delta\beta_\phi(p)$. The graphs appearing here are quite similar to that in Γ , Eq. (60), where now the single line is β_ϕ instead of β_η . The graphical representation of a generic graph is

$$\frac{\delta D}{\delta(\beta_\phi(p))_{ab}} = \text{Diagram} \quad , \quad (72)$$


where p is the momentum on the external line and a and b are the indices on the lines. These indices are to be summed up according to

$$\frac{\delta D}{\delta\beta_\phi(p)} = \sum_{a,b=1}^{N-1} \delta_{ab} \frac{\delta D}{\delta(\beta_\phi(p))_{ab}} .$$

The first few graphs read then

$$\begin{aligned} \frac{\delta D}{\delta\beta_\phi(p)} = & \frac{1}{12} \text{Diagram 1} + \frac{1}{8} \text{Diagram 2} + \frac{1}{16} \text{Diagram 3} + \dots \\ & + \frac{1}{4} \text{Diagram 4} + \frac{1}{8} \text{Diagram 5} + \frac{1}{8} \text{Diagram 6} + \dots \\ & + \frac{1}{4} \text{Diagram 7} + \frac{1}{8} \text{Diagram 8} + \frac{1}{16} \text{Diagram 9} + \dots \\ & + \frac{1}{2} \text{Diagram 10} + \frac{1}{2} \text{Diagram 11} + \dots \end{aligned} \quad (73)$$


We write down the corresponding analytical expression in the form

$$\begin{aligned} \frac{\delta D}{\delta\beta_\phi(p)} = & \text{Tr}_q \beta_\phi(p+q) (\gamma_1 + \gamma_2 + \gamma_3) \\ & + \text{Tr}_q \beta_\eta(p+q) \gamma_4, \end{aligned} \quad (74)$$

where the γ_i 's correspond to the raws in Eq. (73).

For γ_1 we have

$$\gamma_1 = \frac{1}{12} \frac{-6\lambda}{N} \Sigma_\phi^{(1)}(q) \tilde{V}_1 + \sum_{i \geq 2} \frac{1}{2^{n+1}} \left(\frac{-6\lambda}{N} \right)^{n+1} \left(\Sigma_\phi^{(1)}(q) \right)^n \tilde{V}_n,$$

where the \tilde{V}_n result from the summation over the internal indices according to

$$\begin{aligned} \tilde{V}_1 &\equiv \sum V_{aba_1b_1} V_{a_1b_1ab} = \frac{N^2 - 1}{3}, \\ \tilde{V}_n &\equiv \sum V_{aba_1b_1} V_{a_1b_1a_2b_2} \dots V_{a_nb_nab} = \frac{N+1}{3} \left[\left(\frac{N+1}{3} \right)^n + \left(\frac{2}{3} \right)^n (N-2) \right]. \end{aligned}$$

With the notations a , b and c given by Eq. (62) and $\tilde{b} = \frac{2}{N+1}b$ we sum up the geometric series and arrive at

$$\gamma_1 = \frac{-\lambda(N+1)}{2N} \left[\frac{b}{3} + \frac{b^2}{1-b} + (N+2) \left(\frac{\tilde{b}}{3} + \frac{\tilde{b}}{1-\tilde{b}} \right) \right]. \quad (75)$$

With the remaining graphs we proceed in the same manner. For γ_2 we note

$$\begin{aligned} \gamma_2 &= \frac{1}{4} \frac{-6\lambda}{N} \left(\frac{-2\lambda}{N} \right)^2 \Sigma_\eta^{(1)}(q) \Sigma_\phi^{(1)}(q) V_1 \\ &\quad + \frac{1}{8} \left(\frac{-6\lambda}{N} \right)^2 \left(\frac{-2\lambda}{N} \right)^2 \text{Tr}_q \left(\left(\Sigma_\eta^{(1)}(q) \right)^2 \Sigma_\phi^{(1)}(q) V_2 + \Sigma_\eta^{(1)}(q) \left(\Sigma_\phi^{(1)}(q) \right)^2 V_1 \right) + \dots \\ &= \frac{-3\lambda}{N} \frac{N-1}{9} \left(\frac{1}{\epsilon} ab + \frac{1}{\epsilon} a^2b + \frac{1}{\epsilon} ab^2 + \dots \right), \end{aligned} \quad (76)$$

which is essential the same as γ_a in Eq. (64) except for the dependence on ϵ . Summing up we obtain

$$\gamma_2 = \frac{-3\lambda}{N} \frac{N-1}{9} \left(a + aA + \frac{1}{\epsilon} \frac{(2 + \epsilon A + \frac{1}{\epsilon} B) AB}{1 - AB} \right). \quad (77)$$

For γ_3 we have simply

$$\gamma_3 = \frac{-\lambda}{N} (N-1) cC \quad (78)$$

so that taking all together we arrive at

$$\begin{aligned} \frac{\delta D}{\delta \beta_\phi(p)} &= -\frac{\lambda}{N} \left\{ \text{Tr}_q \beta_\phi(p+q) \left[(N+1) \left[\frac{b}{3} + \frac{b^2}{1-b} + (N-2) \left(\frac{\tilde{b}}{3} + \frac{\tilde{b}^2}{1-\tilde{b}} \right) \right] \right. \right. \\ &\quad \left. \left. (N-1) \left[\frac{a}{3} + \frac{1}{3} aA + \frac{1}{3\epsilon} \frac{(2 + A + \frac{1}{\epsilon} B) AB}{1 - AB} \right] \right] \right. \\ &\quad \left. + \text{Tr}_q \beta_\eta(p+q) (N-1) \frac{c^2}{1-c} \right\}, \end{aligned} \quad (79)$$

where $\tilde{b} = \frac{2}{N+1}b$.

References

- [1] Jean Zinn-Justin. *Quantum Field Theory and Critical Phenomena*. Clarendon Press, 1996.
- [2] A. Linde. *Particle Physics and Inflationary Cosmology*. Harwood Academic Publishers, 1990.
- [3] J.I. Kapusta. *Finite-temperature field theory*. Cambridge University Press, 1989.
- [4] N. Tetradis and C. Wetterich. The high temperature phase transition for ϕ^4 theories. *Nucl. Phys.*, B398:659–696, 1993.
- [5] M. Reuter, N. Tetradis, and C. Wetterich. The large n limit and the high temperature phase transition for the ϕ^4 theory. *Nucl. Phys.*, B401:567–590, 1993.
- [6] J. Adams et al. Solving nonperturbative flow equations. *Mod. Phys. Lett.*, A10:2367–2380, 1995.
- [7] I. Montvay and G. Muenster. *Quantum Fields on a Lattice*. Cambridge Univ. Pr. (Cambridge monographs on Mathematical Physics), 1994.
- [8] Z. Fodor, J. Hein, K. Jansen, A. Jaster, and I. Montvay. Simulating the electroweak phase transition in the $su(2)$ higgs model. *Nuclear Physics B*, B439:147–86, 1995.
- [9] K. Takahashi. Perturbative calculations at finite temperatures. *Zeitschrift fur Physik C*, 26:601–13, 1985.
- [10] M. E. Carrington. The effective potential at finite temperature in the standard model. *Phys. Rev.*, D45:2933–2944, 1992.
- [11] P. Arnold. Phase transition temperatures at next-to-leading order. *Phys. Rev. D*, 46:2628–35, 1992.
- [12] Kenzo Ogure and Joe Sato. Critical exponents and critical amplitude ratio of the scalar model from finite-temperature field theory. *Phys. Rev.*, D57:7460–7466, 1998.
- [13] Kenzo Ogure and Joe Sato. Critical properties of the $o(n)$ invariant scalar model using the auxiliary-mass method at finite temperature. *Phys. Rev.*, D58:085010, 1998.
- [14] M. Bordag and V. Skalozub. Phase transition in scalar ϕ^4 theory beyond the super daisy resummations. *J. Phys. A: Math. Gen.*, 34:461–71, 2001.

- [15] John M. Cornwall, R. Jackiw, and E. Tomboulis. Effective action for composite operators. *Phys. Rev.*, D8:2428–2445, 1974.
- [16] M. Bordag and V. Skalozub. On symmetry restoration at finite temperature (scalar case). 1999. hep-th/9908003.
- [17] Per Elmfors. Finite temperature renormalization of the ϕ^3 in six- dimensions and ϕ^4 in four-dimensions models at zero momentum. *Z. Phys.*, C56:601–608, 1992.
- [18] L. Dolan and R. Jackiw. Symmetry behavior at finite temperature. *Phys. Rev.*, D 9:3320–3341, 1974.

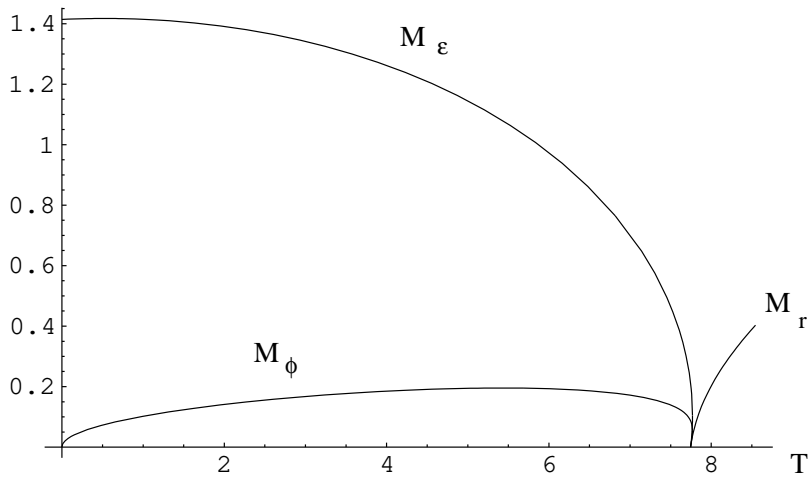
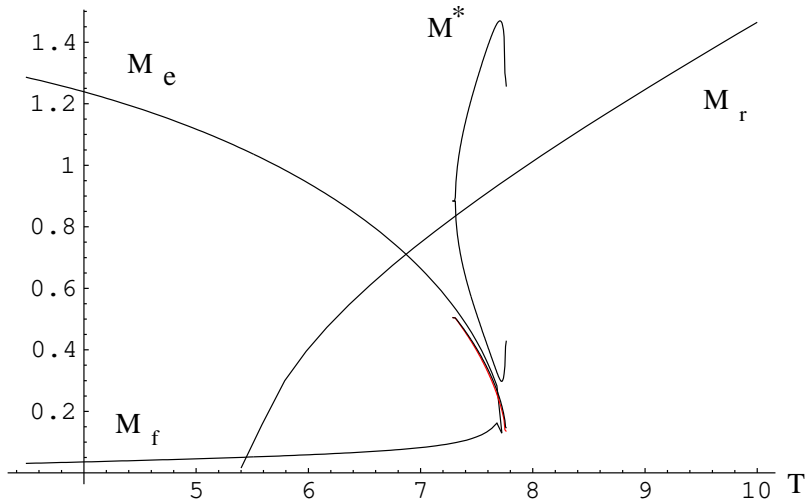


Figure 5: The upper plot shows the numerical solution of the gap equations in the BSDA case as function of the temperature T for $\lambda = 0.1$. Here M_η , M_ϕ are the masses in the broken phase in the minimum of the free energy (the corresponding masses in the maximum are not shown), M_r is the mass in the restored phase and M^* is the mass for the additional solutions. The lower plot shows for comparison the corresponding solution in the SDA case.